New methods for landslide identification and mapping using SAR polarimetry obtained during the PacRim 2000 mission in Taiwan

Kristina R. Czuchlewski and Jeffrey K. Weissel
Columbia University
New York, N.Y., USA
krodrig@ldeo.columbia.edu

Jong-Sen Lee
Naval Research Laboratory
Washington, D.C., USA

Abstract— **We reanalyze PacRim 2000 L-band AIRSAR polarimetry collected over the western foothills of central Taiwan a year after the September 20, 1999 ChiChi earthquake, which produced more than 10,000 landslides. The objective is to explore the utility of SAR data, particularly polarimetry, for identifying and mapping natural hazards like landslides that essentially "resurface" landscapes. An overall goal of this research is to exploit the operational advantages of radars over optical instruments for rapid assessment and response to natural hazards and disasters. Three flightlines of XTI1 AIRSAR were acquired over the two largest landslides, Tsaoling and Mt. Juo-feng-err, as well as hundreds of smaller slides generated by the ChiChi main and aftershocks. We first looked at the relative utility of single channel (co-polarized) SAR, dual polarimetry (co- and cross-polarized channels), and full polarimetry for landslide identification. We found that landslides are very difficult to recognize in fixed polarization SAR data. On the other hand, recognizing hillsides cleared of vegetation by landslides is relatively easy with dual and fully polarimetric data by using cross-polarized and co-polarized cross-sections to provide "radar vegetation indices." Radar target decomposition methods applied to the L-band polarimetry allowed us to explore the changes in scattering mechanisms induced by the action of landsliding on forested hillslopes, and to use derived polarimetric parameters to identify landslides. Application of speckle reduction filters does not degrade the resolution with which small landslides can be mapped. Finally, we explored unsupervised classification methods for efficient mapping of landslides under a rapid response mode of operation. A promising method applied to speckle-filtered data first implements the Freeman and Durden decomposition, separating pixels into three fundamental scattering categories, and then refines the preliminary map using an iterative Wishart classifier.**

Keywords-radar; landslide; filter; speckle; hazard

I. INTRODUCTION

On September 20, 1999, Taiwan experienced its largest earthquake of the 20th Century when at 1:47 am local time a M_w 7.6 earthquake struck the Central Range triggering up to 10,000 landslides. Three flightlines of XTI1 AIRSAR were obtained in September 2000 in central Taiwan over terrain affected by the landslides. Two of the flightlines overflew two kilometer-scale landslides: the Mt. Jou-feng-err landslide north of the epicenter; and the Tsaoling landslide south of the epicenter. The third line overflew the Mt. Jou-feng-err landslide and earthquake epicenter (Fig. 1).

II. METHODOLOGY

We employ L-band (0.25m wavelength) airborne SAR polarimetry to detect surface changes produced by the Tsaoling and Mt. Jou-feng-err landslides. Imaging polarimeters provide a complete description of the scattering properties of radar target materials. The L-Band polarimetry for the Tsaoling landslide (flight ts1223) has been previously analyzed on a per-pixel basis by [1]. They show that the devegetated surfaces of landslide scars are dominated by single-bounce scattering mechanisms, and thus can easily be distinguished from neighboring forested hillslopes characterized by volume scattering. Importantly, water and landslides can be differentiated by polarimetric entropy (H) and average scattering mechanism (alpha) signatures, even though both fall under the general category of surface scatter [2]. Areas affected by landsliding found using the polarimetric classification method agree well with landslide areas derived from available passive/optical remote sensing imagery. In addition, the initial study found that landslides can be identified using dual-polarization SAR systems, like the space-borne Envisat ASAR instrument currently in operation.

We refine the basic methodology to better identify and differentiate landslide source, debris and inundated areas based on their backscatter characteristics. Because radar data are subject to multiplicative and additive noise from speckle, we highlight the edges of large landslides detected by radar scattering by applying a statistical classifier while preserving the dominant polarimetric scattering properties [3]. The algorithm implements the Freeman and Durden decomposition [4], dividing pixels into three different scattering categories and then produces a thematic map with the iterative Wishart classifier [5]. As a follow-up to [1], the new technique is applied to the filtered Mt. Jou-feng-err (flight ts1262) and both unfiltered and filtered Tsaoling datasets (flight ts1223).

This research was supported by National Aeronautics and Space Administration (NASA) grant NAG5-13731.

Report Documentation Page

Form Approved
OMB No. 0704-0188

1. REPORT DATE	2. REPORT TYPE	3. DATES COVERED
25 JUL 2005	**N/A**	**-**

4. TITLE AND SUBTITLE	5a. CONTRACT NUMBER
New methods for landslide identification and mapping using SAR polarimetry obtained during the PacRim 2000 mission in Taiwan	5b. GRANT NUMBER
	5c. PROGRAM ELEMENT NUMBER
6. AUTHOR(S)	5d. PROJECT NUMBER
	5e. TASK NUMBER
	5f. WORK UNIT NUMBER
7. PERFORMING ORGANIZATION NAME(S) AND ADDRESS(ES) **Columbia University New York, N.Y., USA**	8. PERFORMING ORGANIZATION REPORT NUMBER
9. SPONSORING/MONITORING AGENCY NAME(S) AND ADDRESS(ES)	10. SPONSOR/MONITOR'S ACRONYM(S)
	11. SPONSOR/MONITOR'S REPORT NUMBER(S)

12. DISTRIBUTION/AVAILABILITY STATEMENT
Approved for public release, distribution unlimited

13. SUPPLEMENTARY NOTES
See also ADM001850, 2005 IEEE International Geoscience and Remote Sensing Symposium Proceedings (25th) (IGARSS 2005) Held in Seoul, Korea on 25-29 July 2005. , The original document contains color images.

14. ABSTRACT

15. SUBJECT TERMS

16. SECURITY CLASSIFICATION OF:			17. LIMITATION OF ABSTRACT	18. NUMBER OF PAGES	19a. NAME OF RESPONSIBLE PERSON
a. REPORT	b. ABSTRACT	c. THIS PAGE			
unclassified	**unclassified**	**unclassified**	**UU**	**4**	

Standard Form 298 (Rev. 8-98)
Prescribed by ANSI Std Z39-18

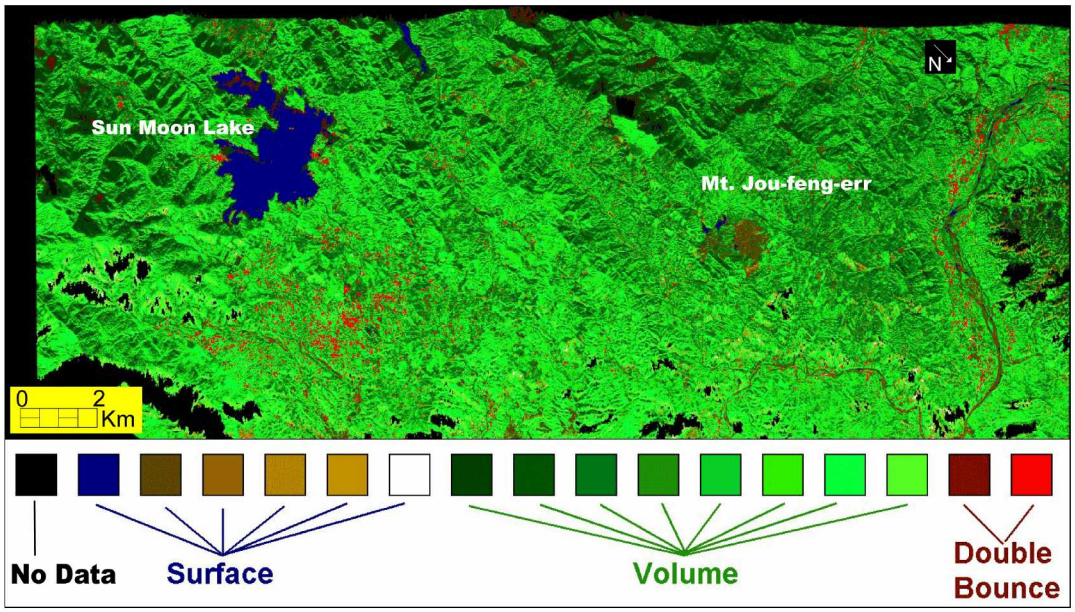

Figure 1. Lee-filtered and classified L-Band AIRSAR flightline (ts1262) over Mt. Jou-feng-err landslide obtained September, 2000.

III. DISCUSSION

A. *Mt. Jou-feng-err*

We first determine if the methodology can rapidly and reliably identify regions of bare surface, water and forest. The processing of the entire AIRSAR swath (Fig. 1) is achieved by applying a 4x4 average to reduce the data for efficient processing. The 4x4 average reduces the speckle noise level such that no further filtering is necessary. Fig. 1 reveals bare, rough surfaces that have experienced landsliding (brown) indicating single bounce surface scattering and classifies the smooth water in Sun Moon lake as surface scattering of low radar returns (blue). The rivers (right hand side of the scene) appear brown suggesting the presence of rougher water from currents or wind disturbances. Forested regions are green from multiple bounce, volume scattering. The red pixels on the edge of the lake, on the banks of the river, and in the main town on the lower left side of the scene arise due to double bounce scattering from buildings.

Comparison between the different passive/optical techniques for landslide mapping is shown in Fig. 2. Fig. 2a shows the surface cover classification of the Mt. Jou-feng-err landslide area [3]. Unlike the classification for the whole scene in Fig. 1, the two small impoundments can not be differentiated from landslides. This is because a small scene (1601x1254) was selected for refined processing to retain the original resolution. The covariance matrices were speckle filtered [5] using the standard deviation to mean ratio of 0.5. Fig. 2a is a cropped area from this small scene. In our algorithm, the classification is based on a cluster scheme derived from the Wishart distribution. Small clusters are forced to merge to a large cluster based on a Wishart distance measure. This process forced the two small lakes to merge with the landslide class. For the whole scene classification, however, the large lake (Sun Moon Lake) provides enough pixels establishing a large enough cluster to retain this class. This problem could be avoided by slightly modifying the classification algorithm.

For comparison, the L-Band polarimetric cross-sections are shown in Fig. 2b as a color composite. This combination identifies variability within the scene between bare surfaces (purple due to higher contribution by hh and vv) and depolarizing surfaces such as vegetation cover (green due to higher contributions by hv). Note that the impounded lake is black because of specular reflection.

The L-Band classification map is compared to optical satellite data over the Mt. Jou-feng-err landslide in Figs. 2c and 2d. Landsat 7 data shown in Fig. 2d were acquired in February, 2001, 5 months after the AIRSAR data and 17 months after the Chi-Chi earthquake. As noted by [1], and despite the coarser resolution of the Landsat 7 data (28.5 m) compared to the AIRSAR data, the location of the landslide area and inundated area are readily identified. Notice vegetation re-growth that occurred between the time of the landslide (best depicted in the IRS panchromatic data of Fig. 2d) and the Landsat datatake, indicated by the green areas in the southwest quadrant of the landslide affected area. Re-vegetation of the landslide debris apron is also apparent from the L-Band polarimetry classification map and cross sections (Figs. 2a and 2b). In the classification map, we observe a higher percentage of green pixels over the debris apron than over the landslide source region.

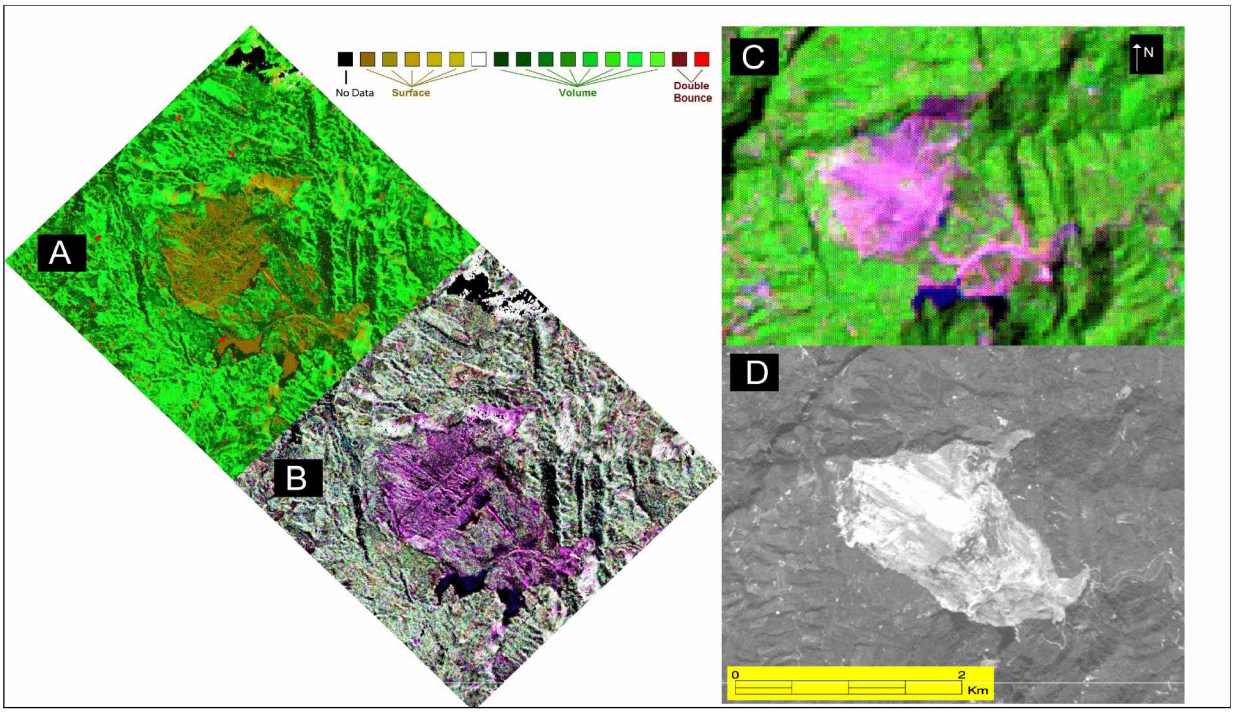

Figure 2. Remote sensing data obtained over Mt. Jou-feng-err landslide which occurred September 20, 1999. (a) Classification map of AIRSAR L-Band polarimetry from technique outlined in [3].(b) RGB false color composite of the L_{hh}, L_{hv}, L_{vv} radar cross section from the AIRSAR L-band polarimetry, (c) Landsat TM (acquired February 2001), short wavelength infrared band 7 (2.08-2.35 μm), near infrared band 4 (0.76-0.90 μm), and visible red band 3 (0.53-0.60 μm) in a RGB false color composite, and (d) IRS visible band panchromatic data acquired October 31, 1999. The IRS and AIRSAR data both have 5m pixels. The Landsat TM has 28.5 m pixels.

The landslide is very well depicted as the high albedo area in the IRS panchromatic data obtained on October 31, 1999, 6 weeks after the earthquake (Fig. 2d). The re-growth of vegetation along the perimeter of the landslide and debris apron (Fig. 2) is significant between the time of AIRSAR and IRS data acquisition rendering it difficult to assess the mapping precision of the AIRSAR analysis.

B. Tsaoling Landslide

In addition to our analysis of the Jou-feng-err slide, we re-examine the Tsaoling landslide using the technique of, [3] (Fig. 3). Fig. 3a shows the IRS data acquisition of October 31, 1999 over the larger of the two landslides. We show this image as a comparison to the three AIRSAR derived maps in Figs. 3b-d. Fig. 3b is the L-band color composite of radar cross sections. As in Fig. 2b, we can readily identify bare surfaces (purple) from vegetated surfaces (green) and locate water based on its low radar returns.

Fig. 3c is the classification result using the original L-band AIRSAR data without speckle filtering. Regions of double bounce, volume and bare surface scattering are easily identified. Water appears as a class of bare surface scattering (blue). To illustrate the effect of speckle filtering, the original data was speckle filtered [5], before applying the classification algorithm. A comparison with Fig. 3d reveals that the application of the speckle filter yields more within class uniformity without compromising the perimeters of the landslides. Note that within the inundated region of the debris apron, pixels that correspond to water (Fig. 3b) are misclassified as volume or double bounce scattering. This is a function of noise received at the antenna being misinterpreted as diffuse scattering.

We also experimented with the P-band data. The results were not as good as the L-band, as expected. P-band microwave with longer wavelength (64 cm) penetrates deeper into vegetated areas inducing surface scattering. This fact causes the landslide pixels to be indistinguishable from vegetation pixels.

IV. CONCLUSION

The classification of bare surfaces vs. forested vs. inundated surfaces agrees well with the results of [1]. The filtering retains the within class uniformity while preserving the edges of the landslides. The use of an unsupervised classification renders empirical thresholds for parameters such as the pedestal height, radar vegetation index and entropy (H) unnecessary.

While [3] validates this technique with two well studied scenes, it is our hope that our results, in addition to their close agreement with the maps shown in by this research, will encourage the remote sensing community to further apply SAR- based algorithm development to hazard mapping.

REFERENCES

[1] Czuchlewski, K.R., J.K. Weissel and Y. Kim, "Polarimetric synthetic aperture radar study of the Tsaoling landslide generated by the Chi-Chi earthquake, Taiwan," J. Geophys. Res., 108(F1), 6006, doi:10.1029/2003JF000037, 2003.

[2] Cloude, S. R., and E. Pottier, "A Review of Target Decomposition Theorems in Radar Polarimetry," IEEE Trans. Geosci. Remote Sens., vol. 34, p.p. 498-518, 1996.

[3] Lee, J.-S., M. R. Grunes, E. Pottier and L. Ferro-Famil, "Unsupervised terrain classification preserving polarimetric scattering characteristics," IEEE Trans. Geosci. and Remote Sens., 42, 722 -731, 2004.

[4] Freeman, A. and S. Durden, "A three-component scattering model for polarimteric SAR data," IEEE Trans. Geosci. Remote Sens., 36, 963-973, 1998.

[5] Lee, J.-S., M.R. Grunes and G. De Grandi, "Polarimetric SAR speckle filtering and its implication for classification," IEEE Trans. Geosci. Remote Sens., 37, 2363-2373, 1999.

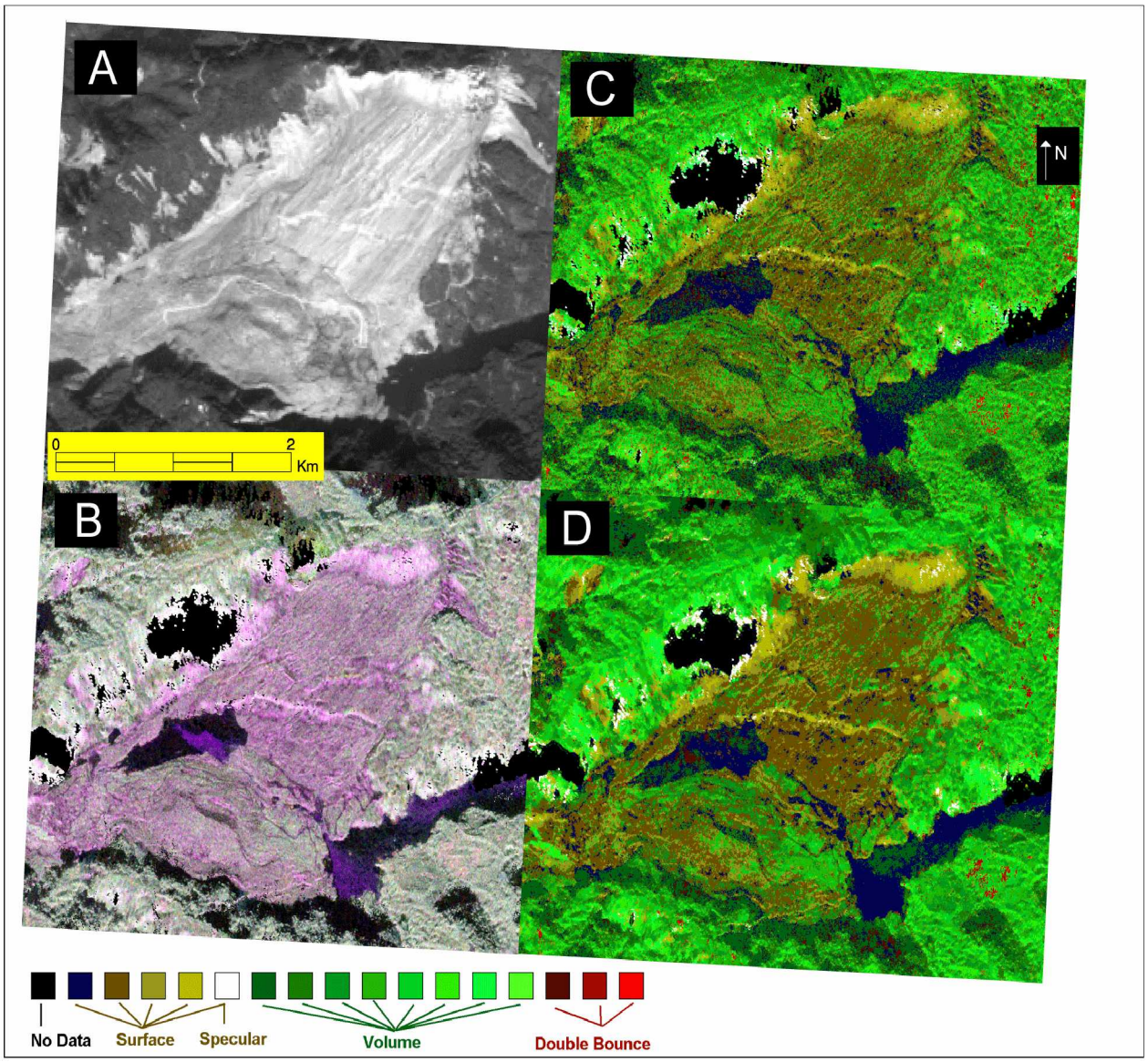

Figure 3. Remote sensing data obtained over Tsaoling landslide. All datasets acquired as in Fig. 2. (a) IRS visible band panchromatic data, (b) RGB false color composite of the L_{hh}, L_{hv}, L_{vv} radar cross section from the AIRSAR L-band polarimetry, (a) unfiltered thematic classification map of AIRSAR data, and (d) filtered classification map of AIRSAR data from technique outlined in [3].